Radiocarbon, Vol 66, Nr 5, 2024, p 989–1005 DOI:10.1017/RDC.2023.72
Selected Papers from the 24th Radiocarbon and 10th Radiocarbon & Archaeology International Conferences, Zurich, Switzerland, 11–16 Sept. 2022.

ATMOSPHERIC CO_2 CARBON ISOTOPE COMPOSITION IN URBAN AND CLEAN AREAS OF THE NORTHERN ADRIATIC COAST OF CROATIA

Andreja Sironić[1] • Emma Hess[2] • Jadranka Barešić[1]* • Tjaša Kanduč[3] • Damir Borković[1] • Ines Krajcar Bronić[1]

[1]Ruđer Bošković Institute, Zagreb, Croatia
[2]Department of Physics (student), University of Rijeka, Rijeka, Croatia,
[3]Department of Environmental Sciences, Jožef Stefan Institute, Ljubljana, Slovenia

ABSTRACT. Over the course of one year (2021), we monitored the carbon isotope composition of atmospheric CO_2 at three locations in Croatia: the Adriatic port city of Rijeka (Cfa climate) and at two rural sites: Gornje Jelenje (Cfb climate) in the vicinity of a main road and clean-air site Parg (Dfb climate). Carbon isotope composition at all sites shows seasonal variation, ranging from –41.3 to 25.2‰ for $\Delta^{14}C$ and from –13.1 to –11.3‰ for $\delta^{13}C$. Rijeka systematically has the lowest and Parg the highest $\Delta^{14}C$, and $\delta^{13}C$ at the sites are not statistically different one from another. The $\Delta^{14}C$ of leaves of deciduous trees reflect the trend of atmospheric $\Delta^{14}C$. Based on the assumption that the investigated area is under the influence of two main sources of CO_2: fossil and natural (sea exchange, biosphere, and undisturbed – clean air atmospheric component) the approximate share of fossil CO_2 in total atmospheric CO_2 has been estimated for Rijeka (2.1 ± 1.3%) and Gornje Jelenje (1.0 ± 0.9%). Comparison of our results with the data from European CO_2 sampling stations indicates strong influence of CO_2 from sea and biosphere. Backward trajectories indicate a possibility of $\Delta^{14}C_{CO2}$ contribution from distant EU nuclear power plants, but movement of air masses should be considered in more detail to confirm this.

KEYWORDS: $\delta^{13}C$, $\Delta^{14}C$, Adriatic Sea, atmospheric CO_2, urban and clean-air site.

INTRODUCTION

The isotopes of carbon, radioactive ^{14}C and stable ^{13}C (as $^{14}C/^{12}C$ and $^{13}C/^{12}C$ ratios, or $\Delta^{14}C$ and $\delta^{13}C$, respectively), are mostly used in global carbon and atmospheric studies, as well as for the study of anthropogenic influence on the environment. Both isotopes originate from natural and anthropogenic sources. Natural ^{14}C production predominantly depends on the Earth's geomagnetic field and solar activity and it varied significantly in the past (Muscheler et al. 2005; Miyake et al. 2012; Mekhaldi et al. 2015; Channell et al. 2018; Heaton et al. 2021). Natural ^{14}C distribution in the Earth's atmosphere was anthropogenically disturbed in 19th century when a decrease of ^{14}C concentration in atmospheric CO_2 ($\Delta^{14}C_{CO2}$) was recorded in tree rings and correlated with the beginning of the Industrial Revolution and the release of ^{14}C free CO_2 into the atmosphere due to fossil fuel combustion (Suess 1955). Similarly, $\delta^{13}C$ of atmospheric CO_2, with pre-industrial value of –7‰, also decreased, since fossil fuels have $\delta^{13}C$ values around –26‰ (Graven et al. 2020; Keeling and Graven 2021). In the 1950s and 1960s, atmospheric ^{14}C concentration suddenly increased due to atmospheric nuclear bomb testing. ^{14}C activity almost doubled in the Northern Hemisphere and reached a peak in 1963 (Nydal and Lövseth 1965), after which it started decreasing due to the Nuclear Test Ban Treaty and CO_2 exchange with other carbon reservoirs, mostly oceans (Levin and Hesshaimer 2000; Hua et al. 2013; Graven et al. 2020; Heaton et al. 2021; Kutchera 2022; Levin et al. 2022). Today, levels of $\Delta^{14}C_{CO2}$ have approached pre-bomb values (Heaton et al. 2021; Hua et al. 2022) and further decrease of ^{14}C concentration is predicted as well as a decrease in $\delta^{13}C$ values stemming from fossil fuel combustion (Heaton et al. 2021; Hua et al. 2022; Levin et al. 2022). The decrease of $\Delta^{14}C_{CO2}$ and $\delta^{13}C_{CO2}$ in the future can be enhanced by the exchange of CO_2 between oceans and the atmosphere (Menviel et al. 2015; Skinner et al. 2017; Keeling and Graven 2021). The oceans may also become a source of ^{14}C release into the atmosphere due to

*Corresponding author. Email: jbaresic@irb.hr

release of bomb ^{14}C from the water column (Gao et al. 2019; Levin et al. 2022). Other sources of man-made ^{14}C, such as various nuclear facilities, can contribute to an increase of $\Delta^{14}C_{CO2}$ locally.

Generally, $\Delta^{14}C_{CO2}$ has a seasonal trend with expected maximum concentration during spring/summer mainly due to vertical mixing between the troposphere and stratosphere (Turnbull et al. 2009; Graven et al. 2020). In the autumn and winter seasons $\Delta^{14}C_{CO2}$ values decrease due to a lack of atmospheric mixing. Locally, the winter $\Delta^{14}C_{CO2}$ minima could be observed in urban (Rakowski et al. 2008; Molnár et al. 2010; Varga et al. 2019) and even clean-air site areas due to fossil fuel burning during heating season (Major et al. 2018). $\delta^{13}C_{CO2}$ also shows seasonality, but for different reason: higher spring/summer values are due to photosynthesis and lower autumn/winter values are due to plant respiration (Turnbull et al. 2009; Graven et al. 2020). Since $\delta^{13}C$ of fresh plants and respired CO_2 are generally similar to that of the fossil fuel, $\delta^{13}C$ cannot be used to differentiate bio from fossil carbon. $\Delta^{14}C_{CO2}$ is monitored by several long-term stations (Levin and Hammer 2021; Levin et al. 2022) of which there are currently 15 stations active in Europe (ICOS 2022). $\delta^{13}C_{CO2}$ is monitored world-wide by the Scripps CO_2 Program (Keeling et al. 2005; Keeling and Graven 2021) and Global Monitoring Laboratory (NOAA – GML 2023; Vaughn et al. 2010).

We present the establishment of three experimental stations for monitoring $\Delta^{14}C_{CO2}$ and $\delta^{13}C_{CO2}$ in the northern coastal area of Croatia: the port of Rijeka and two sites in its surroundings (Gornje Jelenje and Parg). The aim was to determine the influence of fossil fuel combustion on $\Delta^{14}C_{CO2}$ and $\delta^{13}C_{CO2}$ values at different locations with the hypothesis that the urban site is affected by fossil fuel uses. It should be emphasized that there is no previous data on carbon isotopic composition of atmospheric CO_2 in the Croatian coastal area and there are scant data from European coastal areas. European monitoring sites included in the ICOS program are mainly continental (Levin et al. 2022; Scripps CO_2 Program 2022) and the stations included in Scripps CO_2 Program, such as Mauna Loa, Hawaii, are situated on Pacific islands or close to the Arctic and Antarctic (Keeling et al. 2005; Keeling and Graven 2021; Scripps CO_2 Program 2022). A few monitoring programs have analyzed carbon isotopic composition of the atmospheric CO_2 above the oceans collected from boats (Dutta et al. 2006; Longinelli et al. 2012; Gao et al. 2019) and isotopic composition of dissolved inorganic carbon (DIC) (Becker et al. 2016; Gao et al. 2019; Scripps CO_2 Program 2023). The Mace Head (MHD) monitoring station situated on west coast of Ireland is exposed to clean marine air nearly 50% of the time but is also under the influence of polluted air masses from the UK and Europe (Yttri et al. 2019).

SAMPLING AND METHODS

Sampling Sites Characterization

The characteristics of all three sampling locations are summarized in Table 1. Rijeka is the third largest city in Croatia and has the largest seaport, with 128,600 inhabitants and a population density of 2900 inhabitants/km^2. It is located in Primorje-Gorski Kotar County, on the coast of the Kvarner Gulf (Figure 1). The climate of Rijeka is moderately warm and humid with hot summers (Cfa) (Peel et al. 2007; Beck et al. 2018). It is known for the Bora, the cold and dry north-easterly wind (CMHS 2022; Figure 2a) that sometimes gusts at hurricane speeds (160 km/hr). The annual mean air temperature (T) in 2021 was 15.1°C (seasonal variations in Figure 2b), and the total amount of precipitation (P) was 1161 mm (CMHS 2022). The samples

https://doi.org/10.1017/RDC.2023.72 Published online by Cambridge University Press

Table 1 Characteristics of the three sampling locations.

Location	Type	Latitude	Longitude	Alt. (m a.s.l.)	$T_{annual\ mean}$ (°C)	P (mm)
Rijeka	Urban	45°20'13"N	14°26'34"E	0	15.1	1161
Gornje Jelenje	Rural + road	45°21'52"N	14°37'07"E	882	—	—
Parg	Rural/clean	45°35'37"N	14°37'50"E	863	8.4	1586

Figure 1 (a) Map of Europe with Croatia highlighted; (b) position of the sampling area in Croatia; (c) enlarged map of sampling points, and (d) micro location of sampling point in Rijeka

were collected in the center of the city (Figure 1d), near the main railway station, 9 m above ground (0 m a.s.l), on the terrace of an apartment.

Gornje Jelenje is a saddle located 14 km northeast of Rijeka in the foothills of Risnjak National Park and Snježnik Mountain (Figure 1). The area is covered by forests, and the sampling site is located 500 m away from the main road at 882 m a.s.l.; the samples were collected 2 m above the ground. The climate is moderately warm and humid with warm summers (Cfb) (Peel et al. 2007; Beck et al. 2018). Gornje Jelenje is not a CMHS station and there is no meteorological data for this site.

https://doi.org/10.1017/RDC.2023.72 Published online by Cambridge University Press

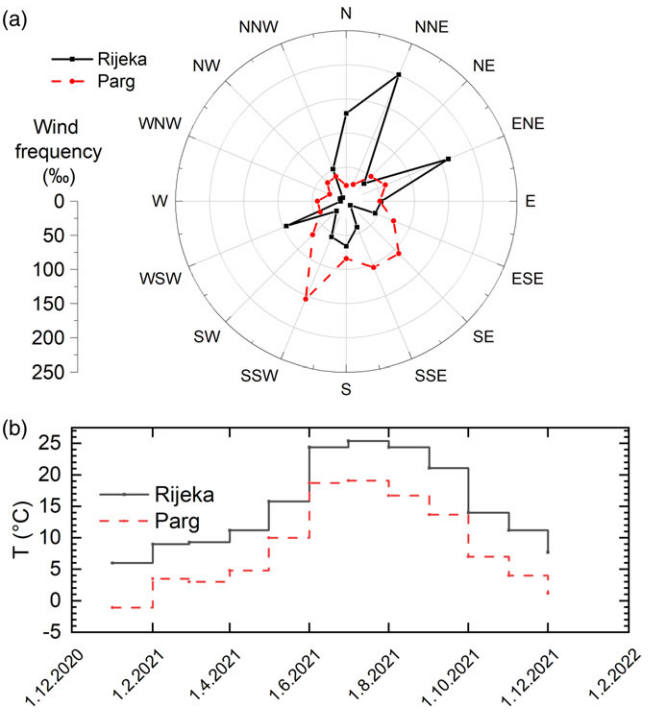

Figure 2 (a) Wind roses for Rijeka and Parg in 2021. (b) Air temperatures for Rijeka and Parg (CMHS 2022).

Parg is a village in Gorski Kotar, 33 km distant from Rijeka. It is located in a wooded, mountainous area far from inhabited zones and roads (Figure 1). The climate is classified as Dfb type (Peel et al. 2007; Beck et al. 2018) with annual mean air temperature in 2021 of 8.4°C (seasonal variations in Figure 2b), and an annual amount of precipitation 1586 mm with snowfall in the winter period and warm summers. The wind that prevails in the area is SW to SE (CMHS 2022, Figure 2a); samples were collected 2 m above the ground.

Sampling Methods

Sampling for atmospheric CO_2 $\Delta^{14}C$ and $\delta^{13}C$ analyses was performed from January 2 to December 28, 2021. Atmospheric CO_2 for $\Delta^{14}C$ analyses was sampled by static absorption method on saturated NaOH in plastic pads as a one-month integrated sample. Absorption occurs under highly alkaline conditions (Dietzel 1997) accompanied by intensive isotope fractionation and the $\delta^{13}C$ of absorbed CO_2 (in form of Na_2CO_3) is not representative for atmospheric CO_2 (Krajcar Bronić et al. 2006). Na_2CO_3 samples were transferred from sampling pads into plastic bottles and thoroughly sealed to avoid isotopic exchange between sample and the atmosphere. For $\delta^{13}C_{CO2}$ analyses, grab air samples were collected by 50 mL plastic syringe and transferred to a 12 mL Labco glass ampoule fitted with a gas-tight septum, flushed using two needles (input and output needle) and filled with air under pressure (Kanduč et al. 2021). Three ampoules were filled per location: at 2 m above ground at Parg and Gornje Jelenje, and 9 m above the ground in Rijeka. These samples were taken at the same sampling heights as the samples for the $\Delta^{14}C$ analyses and stored at standard atmospheric conditions until analysis. Sampling was performed between 2:00 and 5:00 pm.

https://doi.org/10.1017/RDC.2023.72 Published online by Cambridge University Press

The leaves of deciduous trees were collected on August 30, 2021, directly from a plane tree (*Platanus*) in Rijeka and maple trees (*Acer*) in Parg and Gornje Jelenje.

Measurement Methods

The majority of the CO_2 samples and leaf samples were measured in the form of benzene in a Liquid Scintillation Counter Quantulus 1220 (Horvatinčić et al. 2004; Krajcar Bronić et al. 2023). CO_2 was released from Na_2CO_3 by HCl (18%) in an inert N_2 atmosphere and cryogenically purified. The obtained CO_2 was converted to benzene in vacuum synthesis line (Horvatinčić et al. 2004). The leaf samples were carbonized at 650°C and converted to benzene (Horvatinčić et al. 2004; Krajcar Bronić et al. 2023). Accelerator mass spectrometry (AMS) was used in the cases when the sample quantity of absorbed CO_2 was not enough for benzene synthesis. Samples were prepared in the form of graphite targets: CO_2 from Na_2CO_3 was evolved using acid (4% HCl) and reduced to graphite with Zn reduction on Fe powder (Sironić et al. 2013). Graphite samples were measured at the Center for Applied Isotope Studies, University of Georgia (Cherkinsky et al. 2010). Anthracite and SRM 4990C (OxA II) were used as background and reference samples, respectively, for both techniques. All ^{14}C activities were corrected to the date of sampling and defined as $\Delta^{14}C$ (Mook and van der Plicht 1999; van der Plicht and Hogg 2006).

$\delta^{13}C_{CO2}$ from the air samples was determined on the Europa Scientific 20-20 mass spectrometer with the continuous flow IRMS ANCA-TG preparative module at the Jožef Stefan Institute, Ljubljana in Slovenia. Reference material with a known value of $\delta^{13}C_{CO2}$ (–35.4 ± 0.2‰) calibrated to VPDB (Vienna Pee Dee Belemnite) was used. Additionally, as a working standard, natural gas from emission sources in Sicily with a known $\delta^{13}C_{CO2}$ (–0.87 ± –0.20‰) determined at the Istituto Nazionale di geofisica e vulcanologia, manufacturer: gtp-gas.it, (homepage: https://gtp-gas.it/diassido-liquidi-criogenici-i/9) was used. Two-point normalization was performed for CO_2. 0.01 mL of CO_2 (reference gas and working standards) was transferred to Labco ampoules. The whole collected sample was used for $\delta^{13}C_{CO2}$ determination. Because concentrations of CO_2 in air are low, optimal integral peak area (liquid nitrogen cryo trap) was used. Stable isotopes are reported in the δ notation (Coplen 1996) relative to VPDB and measurement uncertainty was between ±0.3 and ±0.7‰.

Estimation of the Fossil CO_2 Component

We estimated the fossil CO_2 share in the Rijeka and Gornje Jelenje sampling sites assuming that Parg as a clean-air site had ^{14}C signal only from natural sources (CO_2 free from fossil fuel influence, biospheric and sea CO_2). Since the shares of the CO_2 natural components were unknown, we assumed that Rijeka and Gornje Jelenje differed from Parg only in fossil CO_2 share, i.e., we approximated biospheric, sea and fossil-free CO_2 components as a background (Levin et al. 2003). This simplification enabled the estimation of fossil CO_2 contribution in Rijeka and Gornje Jelenje from a simple two component mixing relation:

$$a = -1000 \times X + b \times (1 - X)$$

where "a" represents $\Delta^{14}C_{CO2}$ from Rijeka or Gornje Jelenje, "b" represents the background $\Delta^{14}C$ value, –1000‰ is $\Delta^{14}C$ of fossil CO_2, and "X" is the share of fossil CO_2. Such mixing relations are used when data on CO_2 concentration are not available (Piotrowska et al. 2019). As a background $\Delta^{14}C$ values, data from JFJ (Jungfraujoch, Switzerland) station are usually used (Levin et al. 2008). In this paper the $\Delta^{14}C_{CO2}$ values from Parg were used as background,

https://doi.org/10.1017/RDC.2023.72 Published online by Cambridge University Press

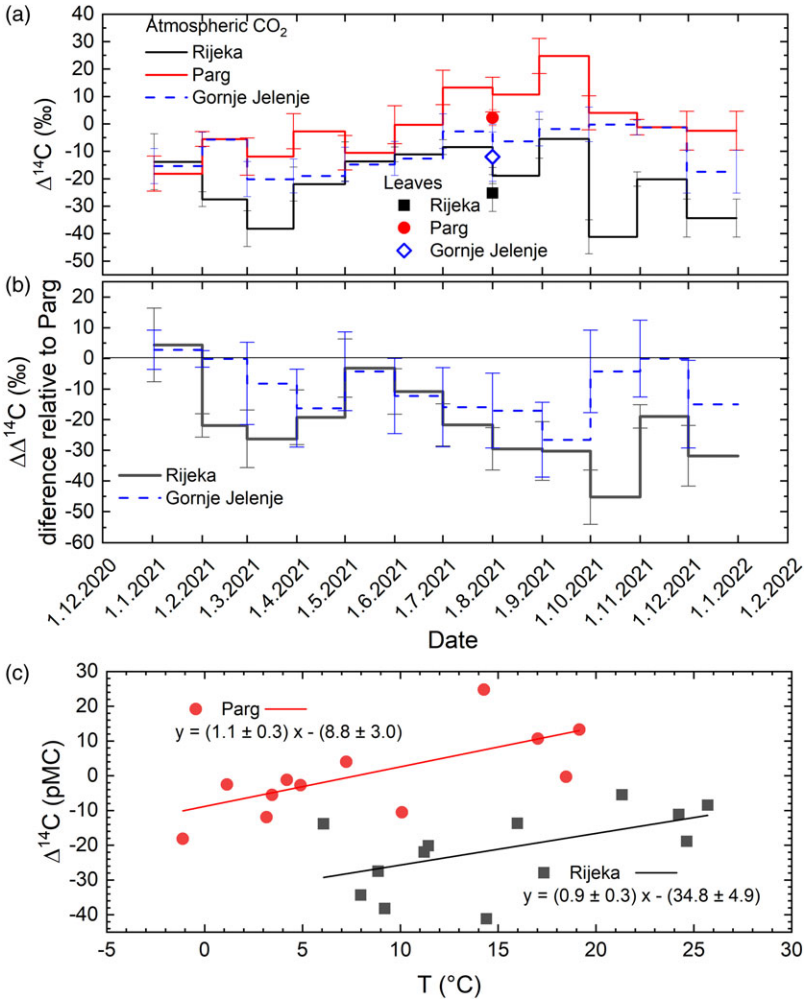

Figure 3 (a) Integrated monthly $\Delta^{14}C$ values at the Rijeka, Gornje Jelenje, and Parg stations for 2021, and for leaves sampled in August 2021 at the respective stations; (b) $\Delta^{14}C$ difference of atmospheric CO_2 for Rijeka and Gornje Jelenje sites compared to the clean-air site Parg; (c) $\Delta^{14}C$ vs. monthly temperature.

and additional calculation was made using the JFJ data from 2020 as data for entire 2021 were not available.

RESULTS AND DISCUSSION

Results of $\Delta^{14}C_{CO2}$ are shown in Figure 3a, while numerical individual data are presented in Table SM1 of supplementary material. For all three locations the data show similar seasonal patterns (Figure 3), with significant correlation with temperature values (Rijeka $r = 0.58$, Parg $r = 0.70$, $p < 0.05$; Figure 3c). $\Delta^{14}C_{CO2}$ mean values (Table 2) show that Gornje Jelenje represents an approximate middle value (–10 ± 8‰) between Rijeka (–22 ± 12‰) and Parg (0 ± 12‰). Tree leaves should reflect $\Delta^{14}C_{CO2}$ values from the spring/summer period (March–September). This is true for the tree leaves from Gornje Jelenje and Parg: their $\Delta^{14}C$

https://doi.org/10.1017/RDC.2023.72 Published online by Cambridge University Press

Table 2 Characteristic carbon isotopic composition of samples from the investigated area, 2021. Individual data are presented in Tables SM1 and SM2.

	$\Delta^{14}C$ (‰) whole year			$\Delta^{14}C$ (‰) March–Sept	$\Delta^{14}C$ (‰) Jan–Feb & Oct–Dec	$\Delta^{14}C$ (‰)
Location	Mean	Min	Max	Mean	Mean	tree leaves
Rijeka	–22 ± 12	–41 ± 6	–6 ± 7	–17 ± 11	–27 ± 11	–25 ± 7
G. Jelenje	–10 ± 8	–20 ± 6	0 ± 6	–11 ± 8	–8 ± 8	–12 ± 9
Parg	0 ± 12	–18 ± 6	25 ± 6	3 ± 13	–5 ± 8	2 ± 3
	$\delta^{13}C$ (‰) whole year			$\delta^{13}C$ (‰) March–Sept	$\delta^{13}C$ (‰) Oct–Dec	
	Mean	Min	Max	Mean	Mean	
Rijeka	–11.6 ± 0.7	–13.1 ± 0.6	–10.7 ± 0.4	–11.2 ± 0.4	–12.2 ± 0.2	
G. Jelenje	–11.5 ± 0.8	–13.0 ± 0.3	–10.6 ± 0.3	–11.0 ± 0.4	–12.4 ± 0.5	
Parg	–11.4 ± 0.7	–12.4 ± 0.3	–10.5 ± 0.3	–11.0 ± 0.5	–12.0 ± 0.2	

values correspond to $\Delta^{14}C_{CO2}$ values for respective periods (Table 2). The leaves from Rijeka show a higher, but statistically insignificant ($z = 0.65$; Table SM3) $\Delta^{14}C$ value compared to the $\Delta^{14}C_{CO2}$ values determined in Rijeka for the spring/summer period (Table 2), and it is more similar to the $\Delta^{14}C_{CO2}$ from winter season. This could be explained by the altitude difference and coastal position of Rijeka, where the budding period generally starts earlier than in the mountain area. The altitude $\Delta^{14}C$ effect has been reported in tree leaves from higher altitudes (Sakurai et al. 2013), but higher $\Delta^{14}C$ values were found at above 3000 m a.s.l. The trend of a $\Delta^{14}C$ increase from the lowest altitude sampling point in Rijeka, to the highest, through Gornje Jelenje to Parg observed in samples of tree leaves, as well as in respective $\Delta^{14}C_{CO2}$ values (Table 2) is the most likely caused by distance from the expected fossil fuel and marine reservoir carbon sources and climatic differences between sites, rather than altitude effect. The increase in $\Delta^{14}C_{CO2}$ between Rijeka and Gornje Jelenje to Parg (from –22‰, –10‰, to 0‰; Table 2) much better fits the increase in air distance from Rijeka (15 km to Jelenje and 32 km to Parg), than the increase in elevation (0 m a.s.l., 882 m a.s.l., and 863 m a.s.l.; Table 1).

The observed decrease of $\Delta^{14}C_{CO2}$ from north to south (clean-air to urban site) could be caused by fossil fuel influence in Rijeka, but this signal is not clear throughout the whole year. In January, the coldest month in 2021 (Figure 2b), $\Delta^{14}C_{CO2}$ values are identical for all three sites (Figure 3a; Table SM1), although it is expected that $\Delta^{14}C_{CO2}$ would be lower in Rijeka due to heating with natural gas and oil. In February, when atmospheric temperatures start to increase, we observed a decrease of $\Delta^{14}C_{CO2}$ in Rijeka and an increase in Gornje Jelenje and Parg. In March, $\Delta^{14}C_{CO2}$ values decreased at all three locations, with the largest difference between Rijeka and Parg (Figure 3b; Table SM3). Starting from May when all three locations had same value, $\Delta^{14}C$ increased peaking in September (Rijeka and Parg), and October (Gornje Jelenje), showing an increasing difference between Parg and the other two locations (Figure 3b). The minimum $\Delta^{14}C_{CO2}$ value was detected in Rijeka in October, but this cannot be explained solely by start of heating season, because November and December temperatures were lower, and $\Delta^{14}C$ values higher than in October (Figure 2b). Rijeka is the main Croatian seaport and a busy tourist destination, so fossil fuel emissions due to heavy traffic should be expected during summer months, but the $\Delta^{14}C$ values were almost identical to those from Gornje Jelenje. During the tourism season in 2021, there were no COVID travel restrictions in Croatia and the number of visitors in the Kvarner area was nearly the same as in 2022 (CBS 2022).

Apart from burning of fossil fuels, the observed $\Delta^{14}C_{CO2}$ fluctuations can be explained by several possible processes. $\Delta^{14}C_{CO2}$ values at all three stations simultaneously started increasing in May, which can be attributed to a penetration of stratospheric air masses enriched with ^{14}C into the troposphere (Levin et al. 2010, 2022; Graven et al. 2012; McDonald et al. 2019; Heaton et al. 2021); this vertical mixing does not occur during the autumn/winter season, resulting in lower $\Delta^{14}C_{CO2}$ values. Wind directions in the investigated areas can also help in data interpretation. Rijeka is under the influence of cold northeast wind that blows from the mountains, i.e., from the direction of Parg and Gornje Jelenje (Figure 2a). Parg is under strong influence of southerly winds, i.e., from the coast toward mountains (Figure 2a). Wind directions imply strong mixing of air masses above Rijeka and Parg, with the influence of the marine air. Due to Marine Reservoir Effect (Faivre et al. 2015) and to the strong vertical mixing processes, especially pronounced in the northern Adriatic during the winter (Vilibić and Supić 2005), surface dissolved inorganic carbon (DIC) is ^{14}C depleted, which is reflected in atmospheric CO_2 (Skinner et al. 2017; Graven et al. 2020; Keeling and Graven 2021); this corresponds to lower $\Delta^{14}C_{CO2}$ values in the autumn/winter period. During summer

https://doi.org/10.1017/RDC.2023.72 Published online by Cambridge University Press

stratification, $\Delta^{14}C_{DIC}$ values are generally higher due to the still present ^{14}C from the bomb peak in marine water column (Fallon et al. 2003; Gao et al. 2019; Guilderson et al. 2021). The presence of bomb peak residue is exhibited in shells from the northern Adriatic ($\Delta^{14}C = 25‰$ in 2013; Peharda et al. 2019). This corresponds to higher $\Delta^{14}C_{CO2}$ during the spring/summer period. The especially high $\Delta^{14}C_{CO2}$ level at Parg could be attributed to the influence of this ^{14}C enriched marine CO_2 that can be transported by strong S and SW winds (Figure 2a), and increased CO_2 outgassing due to high summer temperatures (Figure 2b). Mediterranean influence during the summer has been shown on isotopic composition of precipitation (Vreča et al. 2006; Krajcar Bronić et al. 2020), as well as from backward trajectories for July and September (Stein et al. 2015; Rolph et al. 2017; NOAA – HYSPLIT 2023). The photosynthesis/respiration ratio also has a certain role in $\Delta^{14}C_{CO2}$ dynamics, but it complicates the interpretation of our results as photosynthetic activity during spring/summer that overrides respiration should decrease $\Delta^{14}C_{CO2}$ due to CO_2 consumption, and the respiration, with no photosynthesis (autumn/winter) should increase $\Delta^{14}C_{CO2}$ due to CO_2 production. Nevertheless, photosynthesis vs. respiration could explain the $\Delta^{14}C_{CO2}$ drop in March at all three locations, the most intensive of which was in Rijeka. This corresponded to the observed $\Delta^{14}C$ value of tree leaves from Rijeka and start of budding season earlier compared to the two mountain sites Gornje Jelenje and Parg. Maximum values of $\Delta^{14}C_{CO2}$ in September (Rijeka and Parg) and October (Gornje Jelenje) could be due to soil respiration and CO_2 release into the atmosphere (Trumbore 2000).

Generally, $\Delta^{14}C_{CO2}$ values from urban Rijeka site are the lowest (average value –22 ± 12‰, Table 2) compared to ICOS stations, while values from Gornje Jelenje (average $\Delta^{14}C_{CO2}$ is –10 ± 8‰, Table 2) are comparable to STE (Steinkimmen, Germany, average $\Delta^{14}C_{CO2}$ is –9 ± 6‰, Kubistin et al. 2022a), KRE (Křešín u Pacova, Czechia, average $\Delta^{14}C_{CO2}$ is –8 ± 3‰, Marek et al. 2022). It must be emphasised that clean-air site Parg has higher $\Delta^{14}C_{CO2}$ values (average 0 ± 12‰, Table 2) compared to other EU monitoring stations, but due a huge $\Delta^{14}C_{CO2}$ fluctuation during the year, average value does not show a clear difference. The peak $\Delta^{14}C_{CO2}$ value of 24.8 ± 6.4‰ was observed at Parg in September, and the highest value among the EU stations was 2.6 ± 1.8‰ measured in September at SVB (Svartberget, Sweden, data available until September 2021, Marklund et al. 2022). The ICOS station that could be regarded as most similar to Parg and with data available for the whole of 2021 is KRE, but the maximum $\Delta^{14}C_{CO2}$ value determined for this site was –3.5‰ in August. Other ICOS stations with data available for the whole year are STE, PAL (Pallas, Finland; without data for December; Hatakka 2022) and OPE (Observatoire pérenne de l'environnement, France; without data for December, Ramonet et al. 2022). The maximum $\Delta^{14}C_{CO2}$ values were –0.2‰ measured in August at STE, 1.3‰ measured at PAL in September, and –2.78‰ at HTM (Hyltemossa, Sweden, Heliasz and Biermann 2022), also in September. There are not data for the whole year from the JFJ, but data for 2019 and 2020 show maxima $\Delta^{14}C$ of 6.1 ± 1.5‰ in September and 5.4 ± 1.7‰ in July, respectively (Emmenegger et al. 2022). Data from Mace Head (MHD) would be interesting as this is European maritime station, but $\Delta^{14}C_{CO2}$ values are available only until March 2016. However, a comparison of MHD data from 2015 with the available data for 2015 from JFJ station, show higher summer $\Delta^{14}C_{CO2}$ values at MHD (maximum was 23‰ in August, while maximum $\Delta^{14}C_{CO2}$ for JFJ was 17.4‰ in February). These two values could imply summer ^{14}C sea CO_2 influence onto the atmosphere at MHD, and a similar explanation might be applicable to high summer $\Delta^{14}C_{CO2}$ values at the Parg site. Parg has a $\Delta^{14}C_{CO2}$ range for January–June and October–December, of –18.2‰ to 4.0‰, while between July and September these values are considerably higher within the range from 10.1‰ to 24.8‰. To the best of our knowledge there is no source of anthropogenic ^{14}C in the

https://doi.org/10.1017/RDC.2023.72 Published online by Cambridge University Press

area, since the contribution of $\Delta^{14}C$ from the only nuclear facility in a radius of 100 km from the investigated sites (NPP Krško, Slovenia, NE direction) disappears 15 km from the facility (Krajcar Bronić et al. 2017). Backward trajectories (Stein et al. 2015; Rolph et al. 2017; NOAA – HYSPLIT 2023) indicate travel of air masses from distant areas and that high $\Delta^{14}C_{CO2}$ signals could be transferred from EU nuclear power plants. Investigation of atmospheric pollution in Croatia showed that more than 70% of pollutants have been transferred from other European countries by air masses (Špoler Čanić et al. 2009). However, much more investigation is needed on this topic. As we discussed earlier, apart from seasonal influence of ^{14}C enriched marine CO_2, the high $\Delta^{14}C_{CO2}$ values from Parg could be the result of CO_2 originated from organic matter decomposition. The Parg area is covered mainly by coniferous trees and fallen leaves may be several years or decades old, so the CO_2 resulting from decomposition has higher $\Delta^{14}C$ values compared to the atmosphere of deciduous forest area (Trumbore 2000).

The approximate shares of calculated fossil CO_2 (Table SM5) were 2.1 ± 1.3% at Rijeka and 1.0 ± 0.9% at Gornje Jelenje (yearly averages). The maximum shares were calculated for Rijeka in October (4.5%) and for Gornje Jelenje in September (2.6%) and the minimum, even negative, values of –0.4% (Rijeka) and –0.3% (Gornje Jelenje) in January (Table SM5). The values were also lower compared with data for January from majority of ICOS stations, except the STE ($\Delta^{14}C_{CO2}$ is –15.0‰) and KIT (Karlsruhe, Germany, $\Delta^{14}C_{CO2}$ is –22.3‰, Kubistin et al. 2022b) while other stations had values between –12.9 and 5.6‰. Although the $\Delta^{14}C_{CO2}$ difference between Rijeka and Parg, and Gornje Jelenje and Parg were non-significant for January ($z = 0.37$ and 0.31, respectively, Table SM3), negative shares of fossil CO_2 values indicate the influence of ^{14}C depleted CO_2 at the Parg station, probably transported by SSW wind from the Adriatic Sea (Figure 2a). It is worth mentioning that backward trajectories for January 2021 for three investigated sites as well as for STE and KIT indicate air masses transport from the North Atlantic, detailed investigation on this subject is necessary as well as the ^{14}C analyses of sea DIC to determine the influence of CO_2 form the sea. The calculation with JFJ data as a background (from 2020) give very similar yearly averages for both Rijeka and Gornje Jelenje (Table SM5) without negative values in January, which also implies a source of ^{14}C depleted CO_2 in the Parg site during winter.

The comparison between clean-air sites and industrial areas based on tree ring ^{14}C analyses show higher fossil CO_2 shares in urban European areas compared to Rijeka and Gornje Jelenje: in south-west Slovakia 3.4 ± 1.5% (Kontul' et al. 2020), southern Poland 3.6 ± 0.3% (Rakowski et al. 2005, 2008; Pazdur et al. 2007), and 5.8% in Gliwice, Poland, which is regarded as one of the most fossil CO_2 affected region (Piotrowska et al. 2019). Samples from the Debrecen area, in Hungary, indicate smaller fossil CO_2 contribution in tree leaves (0.9 ± 1.2%) compared to grasses (2.5 ± 2.5%), with higher values in the vicinity of busy crossroads (4.7 ± 0.7% and 9.6 ± 0.7% for tree leaves and grasses, respectively, Varga et al. 2019). Dilution of fossil CO_2 observed in Debrecen at sites away from busy crossroads may be used as an explanation for our data from Rijeka and Gornje Jelenje. Rijeka, although an urban and touristic place, has many city parks that clearly help to remove produced CO_2. This could be valid for the Gornje Jelenje area as well, where the vicinity of the road is heavily forested and therefore rife with photosynthetic activity and CO_2 consumption.

CO_2 for the determination of $\delta^{13}C$ was sampled as a grab sample at the beginning and at the end of the sampling period for $\Delta^{14}C_{CO2}$ determination (Figure 4; Table SM2). $\delta^{13}C_{CO2}$ values have similar seasonal trends for all locations and $\delta^{13}C$ values between all three sites are

https://doi.org/10.1017/RDC.2023.72 Published online by Cambridge University Press

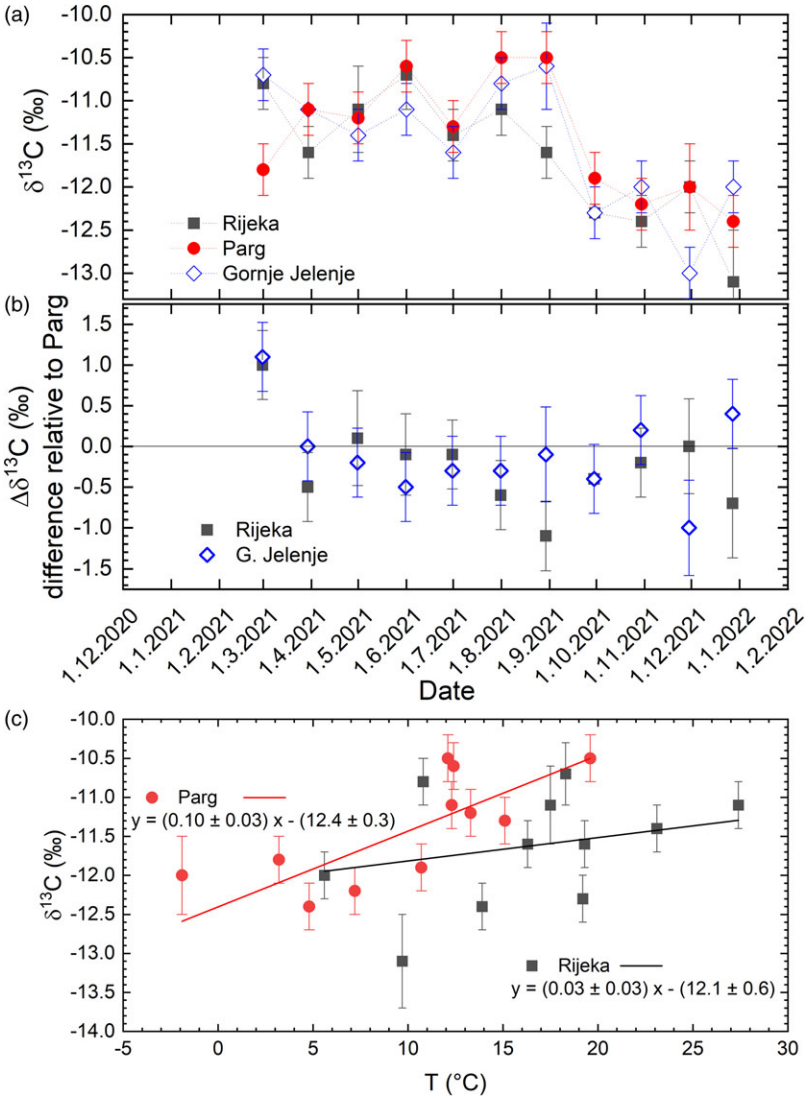

Figure 4 (a) $\delta^{13}C$ in grab samples of atmospheric CO_2 at three locations; (b) $\delta^{13}C$ differences for the Rijeka and Gornje Jelenje sites and the clean-air Parg site; (c) $\delta^{13}C$ vs. temperature.

significantly correlated (R-GJ: $r = 0.66$, $p = 0.025$; R-P: $r = 0.72$, $p = 0.011$; P-GJ: $r = 0.72$, $p = 0.011$). Of the three sites, only the clean-air site Parg is significantly correlated to temperature ($r = 0.77$, $p < 0.02$), implying the predominant influence of natural processes at Parg (photosynthesis with higher $\delta^{13}C$ values and organic matter decomposition with lower $\delta^{13}C$ values). A decreasing trend of $\delta^{13}C$ values from Parg, through Gornje Jelenje to Rijeka is barely visible, and is the most distinguished in minimal values between Parg and the two other sites (Table 2; Table SM4). Although the mean $\delta^{13}C$ values are not significantly different, seasonal fluctuation show differences. Compared to Parg, $\delta^{13}C_{CO2}$ in Rijeka is lower during spring, summer and autumn, but statistically significantly only in September by –1.1‰ ($z = 2.6$) (Figure 4b; Table SM4). $\delta^{13}C_{CO2}$ values at Gornje Jelenje are also lower compared to

https://doi.org/10.1017/RDC.2023.72 Published online by Cambridge University Press

Parg within the same period as Rijeka, but none of these differences are significant. It is interesting that both, Rijeka and Gornje Jelenje, have significantly higher $\delta^{13}C_{CO2}$ for 1‰ (z = 2.4 and 2.6, respectively; Table SM4) compared to Parg in March which corresponds to $\Delta^{14}C_{CO2}$ values drop (Figure 3a) explained earlier as CO_2 photosynthesis uptake. The minima $\delta^{13}C$ values were in January (Parg and Rijeka) and December (Gornje Jelenje) and maxima in September (Parg and Gornje Jelenje) and June (Rijeka) (Figure 4a; Table SM2). The spring and summer $\delta^{13}C$ maxima reflect CO_2 consumption and discrimination of ^{13}C due to photosynthesis. Higher summer values at Parg and Gornje Jelenje compared to Rijeka may be attributed to geographical differences between sites: Parg belongs to the Dfb climate type, Gornje Jelenje to the Cfb while Rijeka to the Cfa climate. The described differences mean that photosynthetic activity at Parg and Gornje Jelenje begins later than in Rijeka. This trend is observed in $\Delta^{14}C$ values of atmospheric CO_2 and tree leaves. Decreasing of $\delta^{13}C$ values from June to the end of the year could be connected to fossil fuel combustion from more intensive traffic in Rijeka, but contribution of soil respiration cannot be neglected and were confirmed by the maximum $\Delta^{14}C$ value in Rijeka in September.

The decrease in $\delta^{13}C$ values at Parg and Gornje Jelenje starts later (in September) reflecting a shift in seasonal activity (start of respiration and decrease in photosynthetic activity). High late summer/autumn $\Delta^{14}C_{CO2}$ values (Figure 3a) at Parg and Gornje Jelenje confirm soil respiration influence.

The $\delta^{13}C_{CO2}$ and $\Delta^{14}C_{CO2}$ values of each investigated site do not correlate to each other, however Parg shows the most similar behavior of $\delta^{13}C_{CO2}$ and $\Delta^{14}C_{CO2}$ values in year (Figures 3a and 4a). This corroborates the assumption that Parg is influenced mostly by natural processes. The $\delta^{13}C$ and $\Delta^{14}C$ differences relative to Parg (Figures 3b and 4b; Table 2) show that Rijeka and Gornje Jelenje are lower than Parg in both values throughout nearly the whole year. All three sites are affected by strong winds and the transport of atmospheric CO_2 depleted in ^{13}C from the sea towards the land, which contributes to the decrease in $\delta^{13}C_{CO2}$ during late autumn/winter period (Figure 4a). The possible sea CO_2 influence are also confirmed by lower winter $\Delta^{14}C_{CO2}$ values (Figure 3a). However, there are no data for seasonal $\delta^{13}C$ and $\Delta^{14}C$ values of DIC from the Adriatic Sea necessary for interpretation of this influence. Additionally, the interpretation of CO_2 sources on the basis of $\delta^{13}C$ is more complicated due to the lack of $\delta^{13}C$ differentiation between $\delta^{13}C_{CO2}$ value derived from fossil fuel combustion and from plant respiration (C3 plants dominate in the Kvarner Gulf) and the lack of data for year 2021 for January and February.

A direct comparison of $\delta^{13}C$ values with other locations in Europe in 2021 is not possible because there are no numerical data available. However, graphical data from GML indicate that all three investigated Croatian sites have lower $\delta^{13}C$ values, ranging from −13.1 ± 0.7‰ to –10.5 ± 0.3‰. For same year, data from HUN (Hegyhatsal, Hungary), and HPB (Hohenpeissenberg, Germany) vary between –8.0‰ during the summer and –9.5‰ during the winter (numerical data were not available, so data were read from the graph from NOAA – GML 2023, Vaughn et al. 2010). The $\delta^{13}C$ data for JFJ station for 2017 has a mean value of –11.4 ± 0.7‰ (Levin and Hammer 2021). The difference in $\delta^{13}C_{CO2}$ from 2017 to 2021 at Mauna Loa, Hawaii, USA (Scripps CO_2 Program 2022) is only 0.06‰ (–8.54 ± 0.02‰ in 2017, –8.60 ± 0.02‰ in 2021) so we may approximate $\delta^{13}C$ in 2021 for JFJ with the one from 2017. There is no significant difference between $\delta^{13}C$ at all three investigated sites and approximate values from JFJ as z values between JFJ and Rijeka, Gornje Jelenje and Parg are 0.24, 0.11, and 0.01 respectively (Table SM6). Similar results of $\delta^{13}C_{CO2}$, from

https://doi.org/10.1017/RDC.2023.72 Published online by Cambridge University Press

–18.0‰ to –6.4‰, with an average of –11.7‰ were obtained in the Velenje Basin (9 locations) in 2011 and were explained by the influence of the largest thermal power plant in Slovenia (Kanduč 2015).

CONCLUDING REMARKS

This paper presents the results of $\delta^{13}C$ and $\Delta^{14}C$ values of atmospheric CO_2 at three experimental sites over a one-year period. The aim was to distinguish CO_2 sources between the clean-air site Parg, the Gornje Jelenje site (in Risnjak National Park, in the vicinity of a main arterial road), and the port city of Rijeka, as Croatia's tourism and seaport center of the northern Adriatic. The obtained results showed the trend of descending $\Delta^{14}C_{CO2}$ from Parg through Gornje Jelenje towards Rijeka (from 0 to –22‰). A similar trend in $\Delta^{14}C$ values was observed in leaves samples collected at the same locations, with decrease from Parg to Rijeka (2 ± 3‰ to –25 ± 7‰, respectively). Based on the assumption that the investigated area is under the influence of three sources of CO_2 (fossil, sea/air exchange and biosphere) and that the difference between Parg and other the two sites is only due to fossil CO_2, the approximate share of fossil CO_2 in atmospheric CO_2 was determined for urban Rijeka site (2.1 ± 1.3%) and Gornje Jelenje (1.0 ± 0.9%) using a Parg as the background level.

$\Delta^{14}C$ values showed a seasonal pattern with lower autumn/winter values and higher spring/summer values, especially at Parg. Seasonality is expected due to natural influences. The Parg summer $\Delta^{14}C$ values reached rather high peaks, not observed in any other EU monitoring station. A possible explanation for the high summer and autumn values is CO_2 enriched with ^{14}C transported from Adriatic Sea and released by soil respiration. The influence of anthropogenically enriched ^{14}C sources cannot be totally excluded, due to the possibility of large air mass transportation from distant nuclear power plants.

There was no significant difference among mean $\delta^{13}C_{CO2}$ values: –11.4 ± 0.7‰ Parg, –11.5 ± 0.8‰ Gornje Jelenje and –11.6 ± 0.7‰ Rijeka. The values are generally quite low, and very similar to those measured at JFJ in 2017. $\delta^{13}C$ values for the station nearest to Croatia, Hegyhatsal, Hungary and Hohenpeissenberg, Germany for 2021 are significantly higher and vary between –8.0‰ during the summer and –9.5‰ during the winter. $\delta^{13}C$ values showed an increase in spring and summer due to photosynthetic discrimination of isotopically lighter CO_2 toward isotopically heavier CO_2. Decrease of $\delta^{13}C$ during winter is possible due to a ^{13}C depleted CO_2 transported from the sea by a strong wind, fossil fuel influence estimated from $\Delta^{14}C$ and to soil respiration. However, differentiation of CO_2 sources on the basis of $\delta^{13}C$ values is not as clear as for $\Delta^{14}C$ values as fossil fuel signal is the same as the fresh C3 biomass signal.

The significant differences in $\delta^{13}C$ between European clean-air site Jungfraujoch and Mauna Loa indicates that it is very important to compare climatologically similar sites, whenever possible.

At the moment, none of the aforementioned possibilities can be clearly distinguished due to the short investigation period. However, it was shown that, in even a such a small experimental area as this one, investigation of isotopic composition of CO_2 has great potential. For future research, clarification of sources of CO_2 in atmosphere other phases (DIC(aq) – CO_2(g)) of carbon cycling (e.g., vegetation, ocean) should be simultaneously traced. The impact of distant ^{14}C sources from nuclear power plants should also be explored in more detail using transport models.

https://doi.org/10.1017/RDC.2023.72 Published online by Cambridge University Press

SUPPLEMENTARY MATERIAL

To view supplementary material for this article, please visit https://doi.org/10.1017/RDC.2023.72

ACKNOWLEDGMENTS

We would like to thank the Croatian Meteorological and Hydrological Service for meteorological data. We would also like to acknowledge the Slovenian Research Agency (ARRS) for Program funding P1-0143: "Cycling of substances in the environment, mass balances, modelling of the environmental processes and risk assessment." We would also like to give special thanks to Stojan Žigon and Anita Rajtarić for their technical support in the laboratory. Finally, we would like to express gratitude to the two anonymous reviewers for their constructive comments, and to Prof. Zvjezdana Bencetić Klaić for fruitful discussion. The authors gratefully acknowledge the NOAA Air Resources Laboratory (ARL) for the provision of the HYSPLIT transport and dispersion model and/or READY website (https://www.ready.noaa.gov) used in this publication.

REFERENCES

Beck HE, Zimmermann NE, McVicar TR, Vergopolan N, Berg A, Wood EF. 2018. Data descriptor: present and future Köppen-Geiger climate classification maps at 1-km resolution. Scientific Data 5:180214. doi: 10.1038/sdata.2018.214

Becker M, Andersen N, Erlenkeuser H, Humphreys MP, Tanhua T, Körtzinger A. 2016. An internally consistent dataset of ^{13}C-DIC in the North Atlantic Ocean – NAC13v1. Earth System Science Data 8:559–70. doi: 10.5194/essd-8-559-2016

CBS (Croatian Bureau of Statistics). 2022. https://podaci.dzs.hr/en/statistics/tourism/. Accessed Dec. 14, 2022.

Channell JET, Hodell DA, Crowhurst SJ, Skinner LC, Muscheler R. 2018. Relative paleointensity (RPI) in the latest Pleistocene (10–45 ka) and implications for deglacial atmospheric radiocarbon. Quaternaty Science Reviews 191:57–72.

Cherkinsky AE, Culp RA, Dvoracek DK, Noakes JE. 2010. Status of the AMS facility at the Center for Applied Isotope Studies, Universiy of Georgia. Nuclear Instruments and Methods in Physics Research B 268 (7–8):867–70.

CMHS (Croatian Meteorological and Hydrological Service). 2022. Data obtained Dec. 6, 2022.

Coplen TB. 1996. New guidelines for reporting stable hydrogen, carbon, and oxygen isotope-ratio dana. Geochimica et Cosmochimica Acta 60(17): 3359–3360.

Dietzel M. 1997. Hydrogeochemische und isotopenchemische Prozesse bei der Aufloesung von Karbonatgestein und bei der Abscheidung von Calcit. In: Geochemie und Umwelt. Berlin: Springer-Verlag. p. 381–393.

Dutta K, Bhushan R, Somayajulu BLK, Rastogi N. 2006. Inter-annual variation in atmospheric Δ^{14}C over the Northern Indian Ocean. Atmospheric Environment 40(24):4501–4512.

Emmenegger L, Leuenberger M, Steinbacher M. 2022. ICOS ATC/CAL ^{14}C Release, Jungfraujoch (5.0 m), 2016-01-04–2021-06-13, ICOS RI, https://hdl.handle.net/11676/plRnhjjPPT-nej6j13nh63rI. Accessed Dec. 17, 2022.

Faivre S, Bakran-Petricioli T, Barešić J, Horvatinčić N. 2015. New data on the marine radiocarbon reservoir effect in the Eastern Adriatic based on pre-bomb marine organisms from the intertidal zone and shallow sea. Radiocarbon 57(4): 527–538.

Fallon SJ, Guilderson TP, Caldeira K. 2003. Carbon isotope constraints on vertical mixing and air-sea CO_2 exchange. Geophysical Research Letters 30:2289. doi: 10.1029/2003GL018049

Gao P, Liping Z, Kexin L, Xiaomei X. 2019. Radiocarbon in the maritime air and sea surface water of the South China sea. Radiocarbon 61(2):461–472. doi: 10.1017/RDC.2018.100

Graven HD, Guilderson TP, Keeling RF. 2012. Observations of radiocarbon in CO_2 at seven global sampling sites in the Scripps flask network: analysis of spatial gradients and seasonal cycles. Journal of Geophysical Research 117(D02303). doi: 10.1029/2011JD016535.

Graven HD, Keeling RF, Rogelj J. 2020. Changes to carbon isotopes in atmospheric CO_2 over the Industrial Era and into the future. Global Biogeochemical Cycles 34(11):e2019GB006170. doi: 10.1029/2019GB006170

Guilderson TP, Schrag DP, Druffel ERM, Reimer RW. 2021. Postbomb subtropical North Pacific

surface water radiocarbon history. Journal of Geophysical Research: Oceans 126. e2020JC01 6881. doi: 10.1029/2020JC016881

Hatakka J. 2022. ICOS ATC/CAL ^{14}C Release, Pallas (12.0 m), 2017-12-14–2021-11-10, ICOS RI. https://hdl.handle.net/11676/FgmSRF_tny15D_apTlggM30r

Heaton TJ, Bard E, Bronk Ramsey C, Butzin M, Köhler P, Muscheler R, Reimer PJ, Wacker L. 2021. Radiocarbon: a key tracer for studying the Earth's dynamo, climate system, carbon cycle and Sun. Science 374:eabd7096. doi: 10.1126/science.abd7096

Heliasz M, Biermann T. 2022. ICOS ATC/CAL ^{14}C Release, Hyltemossa (150.0 m), 2015-09-23–2021-11-10, ICOS RI. https://hdl.handle.net/11676/7mdO4oo6IOOzm2VyfYdVCxgP

Horvatinčić N, Barešić J, Krajcar Bronić I, Obelić B. 2004. Measurement of low ^{14}C activities in a liquid scintillation counter in the Zagreb Radiocarbon Laboratory. Radiocarbon 46(1):105–116.

Hua Q, Barbetti M, Rakowski AZ. 2013. Atmospheric radiocarbon for the period 1950–2010. Radiocarbon 55(4):2059–2072.

Hua Q, Turnbull J, Santos G, Rakowski A, RS, De Pol-Holz R, Hammer S, Lehman SJ, Levin I, Miller JB, Palmer JG, Turney CSM. 2022. Atmospheric radiocarbon for the period 1950–2019. Radiocarbon 64(4):723–745. doi: 10.1017/RDC.2021.95

ICOS. 2022. Icos-cp.eu 2022. https://data.icos-cp.eu/portal/#%7B%22filterCategories%22%3A%7B%22project%22%3A%5B%22icos%22%5D%2C%22level%22%3A%5B1%2C2%5D%2C%22stationclass%22%3A%5B%22ICOS%22%5D%2C%22valType%22%3A%5B%22c14MixingRatioPpm%22%5D%7D%7D, accessed 17 Dec 2022

Kanduč T. 2015. Isotopic composition of carbon in atmospheric air; use of a diffusion model at the water/atmosphere interface in Velenje Basin. Geologija 58(1):35–46. doi: 10.5474/geologija.2015.002

Kanduč T, Sedlar J, Novak R, Zadnik I, Jamnikar S, Verbovšek T, Grassa F, Rošer J. 2021. Exploring the 2013-2018 degassing mechanism from the Pesje and Preloge excavation fields in the Velenje Coal basin, Slovenia: insights from molecular composition and stable isotopes. Isotopes in Environmental and Health Studies 57(6): 585–609.

Keeling CD, Piper SC, Bacastow RB, Wahlen M, Whorf TP, Heimann M, Meijer HA. 2005. Atmospheric CO_2 and $^{13}CO_2$ exchange with the terrestrial biosphere and oceans from 1978 to 2000: observations and carbon cycle implications. In: Ehleringer JR, Cerling TE, Dearing MD, editors. A history of atmospheric CO_2 and its effects on plants, animals, and ecosystems. New York: Springer Verlag. p. 83–113.

Keeling RF, Graven HD. 2021. Insights from time series of atmospheric carbon dioxide and related tracers. Annual Review of Environment and Resources 46:85–110. doi: 10.1146/annurev-environ-012220-125406.

Kontul' I, Svetlik I, Povinec PP, Pachnerova Brabcova K, Molnár M. 2020. Radiocarbon in tree rings from a clean air region in Slovakia. Journal of Environmental Radioactivity 218:106237. doi.org/10.1016/j.jenvrad.2020.106237

Krajcar Bronić I, Breznik B, Volčanšek A, Barešić B, Borković D, Sironić A, Horvatinčić A, Obelić B, Lovrenčić Mikelić I. ^{14}C activity in the atmosphere and biological samples in the vicinity of the Krško nuclear power plant – 10 years of experience. In: Radolić V, Poje Sovilj M, Krajcar Bronić I, ed. Proceedings of the 11th symposium of the Croatian Radiation Protection Association (CRPA), April 5–7, 2017, Osijek, Croatia; Zagreb CRPA; 2017. p. 231–237. In Croatian with English abstract.

Krajcar Bronić I, Barešić J, Borković D, Sironić A, Lovrenčić Mikelić I, Vreča P. 2020. Long-Term Isotope Records of Precipitation in Zagreb, Croatia. Water 12:226. doi: 10.3390/w12010226.

Krajcar Bronić I, Sironić A, Barešić J. 2023. Validation of carbonization as a part of benzene synthesis for radiocarbon measurement. Radiation Physics and Chemistry 204:110721. doi: 10.1016/j.radphyschem.2022.110721

Krajcar Bronić I, Vreča P, Horvatinčić N, Barešić J, Obelić B. 2006. Distribution of hydrogen, oxygen and carbon isotopes in the atmosphere of Croatia and Slovenia. Archives of Industrial Hygiene and Toxicology 57:23–29.

Kubistin D, Plaß-Dülmer C, Arnold S, Kneuer T, Lindauer M, Müller-Williams J. 2022a. ICOS ATC/CAL ^{14}C Release, Steinkimmen (252.0 m), 2019-07-13–2022-01-30, ICOS RI. https://hdl.handle.net/11676/_szD6xqYJD6folY4JFGooV5C

Kubistin D, Plaß-Dülmer C, Arnold S, Kneuer T, Lindauer M, Müller-Williams J, Schumacher M. 2022b. ICOS ATC/CAL ^{14}C Release, Karlsruhe (200.0 m), 2018-02-01–2021-09-20, ICOS RI. https://hdl.handle.net/11676/-VQTSnP6A5kOF8pgILElKsiA

Kutchera W. 2022. The versatile uses of the ^{14}C bomb peak. Radiocarbon 64:1295–1308. doi: 10.1017/RDC.2022.13

Levin, I, Hammer S. 2021. Supplementary data to Levin et al. (2021), Radiocarbon in Global Tropospheric Carbon Dioxide. https://doi.org/10.18160/K6P6-WBH5. Accessed Dec. 15, 2022.

Levin I, Hammer S, Kromer B, Meinhardt F. 2008. Radiocarbon observations in atmospheric CO_2: determining fossil fuel CO_2 over Europe using Jungfraujoch observations as background. Science of the Total Environment 391(2–3): 211–216. doi: 10.1016/j.scitotenv.2007.10.019

Levin I, Hammer S, Kromer B, Preunkert S, Weller R, Worthy DE. 2022. Radiocarbon in global tropospheric carbon dioxide. Radiocarbon 64(4):781–791. doi: 10.1017/RDC.2021.102

https://doi.org/10.1017/RDC.2023.72 Published online by Cambridge University Press

Levin I, Hesshaimer V. 2000. Radiocarbon—a unique tracer of global carbon cycle dynamics. Radiocarbon 42(1):69–80.

Levin I, Kromer B, Schmidt M, Sartorius H. 2003. A novel approach for independent budgeting of fossil fuels CO_2 over Europe by $^{14}CO_2$ observations. Geophysical Research Letters 30(23):2194. doi: 10.1029/2003GL018477

Levin I, Naegler T, Kromer B, Diehl M, Francey RJ, Gomez-Pelaez AJ, Steele LP, Wagenbach D, Weller R, Worthy DE. 2010. Observations and modelling of the global distribution and long-term trend of atmospheric $^{14}CO_2$. Tellus B 62(1):26–46. doi: 10.1111/j.1600-0889.2009.00446.x

Longinelli A, Giglio F, Langone L, Moggio L, Ori C, Selmo E, Sgavetti M. 2012. Atmospheric CO_2 concentrations and $\delta^{13}C$ values between New Zealand and Antarctica, 1998 to 2010: some puzzling results. Tellus B: Chemical and Physical Meteorology 64(1):17472. doi: 10.3402/tellusb.v64i0.17472

Major I, Haszpra L, Rinyu L, Futó I, Bihari A, Hammer S, Jull AJT, Molnár M. 2018. Temporal variation of atmospheric fossil and modern CO_2 excess at a Central European rural tower station between 2008 and 2014. Radiocarbon 60(5):1285–1299. doi: 10.1017/RDC.2018.79

Marek M, Vítková G, Komínková K. 2022. ICOS ATC/CAL ^{14}C Release, Křešín u Pacova (250.0 m), 2017-03-29–2022-01-19, ICOS RI. https://hdl.handle.net/11676/clkf93Q6SDcNBwpXVzwpOwaO

Marklund P, Ottosson-Löfvenius M, Smith P. 2022. ICOS ATC/CAL ^{14}C Release, Svartberget (150.0 m), 2016-02-09–2021-09-29, ICOS RI. https://hdl.handle.net/11676/v_0FrRLGoYWWMB0to2IaGV4g accessed December 17, 2022.

McDonald L, Chivall D, Miles D, Bronk Ramsey C. 2019. Seasonal variations in the ^{14}C content of tree rings: influences on radiocarbon calibration and single-year curve construction. Radiocarbon 61(1):185–194. doi: 10.1017/RDC.2018.64

Mekhaldi F, Muscheler R, Adolphi F, Aldahan A, Beer J, McConnell JR, et al. 2015. Multiradionuclide evidence for the solar origin of the cosmic-ray events of AD 774/5 and 993/4. Nature Communications 6:8611

Menviel L, Mouchet A, Meissner KJ, Joos F, England MH. 2015, Impact of oceanic circulation changes on atmospheric $\delta^{13}CO_2$. Global Biogeochemical Cycles 29:1944–1961. doi: 10.1002/2015GB005207

Miyake F, Nagaya K, Masuda K, Nakamura T. 2012. A signature of cosmic-ray increase in AD 774–775 from tree rings in Japan. Nature 486:240–242.

Molnár M, Major I, Haszpra L, Svetlik I, Svingor É, Veres M. 2010. Fossil fuel CO_2 estimation by atmospheric ^{14}C measurement and CO_2 mixing ratios in the city of Debrecen, Hungary. Journal of Radioanalytical and Nuclear Chemistry 286:471–476. doi: 10.1007/s10967-010-0791-2

Mook WG, van der Plicht J. 1999. Reporting ^{14}C activities and concentrations. Radiocarbon 41(3):227–239.

Muscheler R, Beer J, Kubik PW, Synal H-A. 2005. Geomagnetic field intensity during the last 60,000 years based on ^{10}Be and ^{36}Cl from the Summit ice cores and ^{14}C. Quaternary Science Reviews 24:1849–1860.

NOAA HYSPLIT. 2023. https://www.ready.noaa.gov/hypub-bin/trajasrc.pl. Accessed May 9, 2023.

NOAA – GML. 2023. https://gml.noaa.gov/dv/site/. Accessed April 25, 2023.

Nydal R, Lövseth K. 1965. Distribution of radiocarbon from nuclear tests. Nature 206:1029–1031.

Pazdur A, Nakamura T, Pawelczyk S, Pawlyta J, Piotrowska N, Rakowski A, Sensula B, Szczepanek M. 2007. Carbon isotopes in tree rings: climate and the Suess effect interferences in the last 400 years. Radiocarbon 49(2):775–788.

Peel MC, Finlyanson BL, McMahon TA. 2007. Updated world map of the Köppen-Geiger climate classification. Hydrol. Earth System Science 11:1633–1644.

Peharda M, Sironić A, Markulin K, Jozić S, Borković D, Andersson C. 2019. The bivalve glycymeris pilosa as an archive of ^{14}C in the Mediterranean Sea. Radiocarbon 61(2):599–613. doi: 10.1017/RDC.2018.146

Piotrowska N, Pazdur A, Pawełczyk S, Rakowski AZ, Sensuła B, Tudyka K. 2019. Human activity recorded in carbon isotopic composition of atmospheric CO_2 in Gliwice urban area and surroundings (southern Poland) in the years 2011–2013. Radiocarbon 62(1):141–56. doi: 10.1017/RDC.2019.92

Rakowski AZ, Kuc T, Nakamura T, Pazdur A. 2005. Radiocarbon concentration in urban area. Geochronometria 24:63–68.

Rakowski AZ, Nakamura T, Pazdur A. 2008. Variations of anthropogenic CO_2 in urban area deduced by radiocarbon concentration in modern tree rings. Journal of Environmental Radioactivity 99(10):1558–1565.

Ramonet M, Conil S, Delmotte M, Laurent O. 2022. ICOS ATC/CAL ^{14}C Release, Observatoire pérenne de l'environnement (120.0 m), 2015-09-28–2021-11-22, ICOS RI. https://hdl.handle.net/11676/llsaJzNxT8jv_k_dN2oSVhf9

Rolph G, Stein A, Stunder B. 2017. Real-time Environmental Applications and Display sYstem: READY. Environmental Modelling & Software 95:210–228. doi: 10.1016/j.envsoft.2017.06

Sakurai H, Tokanai F, Kat K, Takahashi Y, Sato T, Kikuchi S, Tavera W. 2013. Latest ^{14}C concentrations of plant leaves at high altitudes in the northern and southern hemispheres: vertical stability of local Suess effect. Radiocarbon 55(3):1573–1579. doi: 10.1017/S0033822200048499

Scripps CO2 Program. 2022. https://scrippsco2.ucsd.edu/data/atmospheric_co2/mlo.html. Accessed Dec. 17, 2022.

Scripps CO2 Program. 2023. https://scrippsco2.ucsd.edu/data/seawater_carbon/ocean_time_series.html. Accessed May 3, 2023.

Sironić A, Krajcar Bronić I, Horvatinčić N, Barešić J, Obelić B, Felja I. 2013. Status report on the Zagreb radiocarbon laboratory—AMS and LSC results of VIRI intercomparison samples. Nuclear Instruments and Methods in Physics Research B 294:185–188. doi: 10.1016/j.nimb.2012.01.048.

Skinner LC, Primeau F, Freeman E, de la Fuente M, Goodwin PA, Gottschalk E, Huang E, McCave IN, Noble TL, Scrivner AE. 2017. Radiocarbon constraints on the glacial ocean circulation and its impact on atmospheric CO_2. Nature Communications 8:16010. doi: 10.1038/ncomms16010

Suess H E. 1955. Radiocarbon concentration in modern wood. Science 122(3166):415–417. doi: 10.1126/science.122.3166.415.b

Stein AF, Draxler RR, Rolph GD, Stunder BJB, Cohen MD, Ngan F. 2015. NOAA's HYSPLIT atmospheric transport and dispersion modelling system. Bulletin of the American Meteorological Society 96:2059–2077. doi: 10.1175/BAMS-D-14-00110.

Špoler Čanić K, Vidič S, Bencetić Klaić Z. 2009. Precipitation chemistry in Croatia during the period 1981–2006. Journal of Environmental Monitoring 11:839–851. doi: 10.1039/b816432k

Trumbore S. 2000. Age of soil organic matter and soil respiration: radiocarbon constraints on belowground c dynamics. Ecological Applications 10(2):399–411.

Turnbull J, Rayner P, Miller J, Naegler T, Ciais P, Cozic A. 2009. On the use of $^{14}CO_2$ as a tracer for fossil fuel CO_2: quantifying uncertainties using an atmospheric transport model. Journal of Geophysical Research 114:D22302. doi: 10.1029/2009JD012308

van der Plicht J, Hogg A. 2006. A note on reporting radiocarbon results and discussion. Quaternary Geochronology 1:237–240.

Varga T, Barnucz P, Major I, Lisztes-Szabó Z, Jull AJT, László E, Pénzes J, Molnár M. 2019. Fossil carbon load in urban vegetation for Debrecen, Hungary. Radiocarbon 61(5):1199–210. doi: 10.1017/RDC.2019.81

Vaughn BH, Evans CU, White JWC, Still CJ, Masarie KA, Turnbull J. 2010. Global network measurements of atmospheric trace gas isotopes. In: West JB, et al., editors. Isoscapes: understanding movement, pattern, and process on earth through isotope mapping. Springer Science+Business Media B.V. Za NOAA GML. doi: 10.1007/978-90-481-3354-3_1

Vilibić I, Supić N. 2005. Dense water generation on a shelf: the case of the Adriatic Sea. Ocean Dynamics 55(5):403–415. doi: 10.1007/s10236-005-0030-5

Vreča P, Krajcar Bronić I, Horvatinčić N, Barešić J. 2006. Isotopic characteristics of precipitation in Slovenia and Croatia: comparisom of continental and maritime stations. Journal of Hydrology 330:457–469.

Yttri KE, Simpson D, Bergström R, Kiss G, Szidat S, et al. 2019. The EMEP Intensive Measurement Period campaign, 2008–2009: characterizing carbonaceous aerosol at nine rural sites in Europe. Atmospheric Chemistry and Physics 19:4211–4233. doi: 10.5194/acp-19-4211-2019

https://doi.org/10.1017/RDC.2023.72 Published online by Cambridge University Press